Macromolecules
Article
Cite This: *Macromolecules* XXXX, XXX, XXX−XXX
pubs.acs.org/Macromolecules

Helical Spin Polymer with Magneto-Electro-Optical Activity

Masashi Otaki and Hiromasa Goto*

Department of Materials Science, Faculty of Pure and Applied Sciences, University of Tsukuba, Tsukuba, Ibaraki 305-8573, Japan

Supporting Information

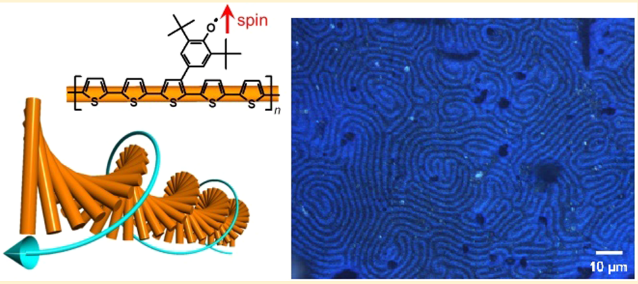

ABSTRACT: A chiral π-conjugated polymer bearing a stable radical side group was synthesized by electrochemical polymerization in a cholesteric liquid crystal. The polymer thus obtained shows paramagnetism as well as electro- and optical activity. The polymer exhibits a one-handed helical spin order owing to the one-handed helix of the main chain and the stable radical side groups. This helical spin order endows the polymer with magneto-optical activity. In situ optical absorption and circular dichroism (CD) measurements during cyclic voltammetry analysis were used to investigate the electroactive chirality of the polymer. Optically active polarons (radical cations) as charge carriers were observed by CD and electron-spin resonance (ESR) measurements. Furthermore, the optical ellipticity of the polarons was found to be tunable using an electric field. The ESR analysis showed that the *g*-value of the phenoxy radicals on the polymer is 2.00403, whereas the *g*-value of the polarons in the main chain is 2.0025, indicating that the phenoxy radical side groups are independent of the polarons in terms of magnetic behavior. CD spectroscopy measurements revealed that the phenoxy radicals exist in a chiral environment. Thus, we successfully obtained a chiral magnetic conjugated polymer using liquid crystal imprinting polymerization. This method is a new approach for the preparation of chiral organic magnets.

INTRODUCTION

Conjugated polymers currently receive considerable research interest owing to their characteristic optical, electrochemical, and magnetic properties, all of which can be modulated by rational design and control of the polymer structure. The application of these materials in organic transistors,[1] sensors,[2] electrochromic devices,[3,4] and organic solar cells[5] has promoted the development of new polymer synthesis and processing methods. In particular, following the development of organic conductors, organic magnets consisting of π-conjugated materials have been proposed as the next generation of synthetic metals. Several strategies for the synthesis of ferromagnetic polymers have been explored. For example, Nishide et al. have reported extensive research on polyacetylene-based[6,7] and polyphenylenevinylene-based[8−10] polyradicals, which were prepared by exploiting the high-spin states available via intramolecular through-bond magnetic ordering upon π-conjugation. According to these reports, the formation of planar and cross-linked polyradical frameworks on π-conjugated backbones are important factors for spin parallel alignment.[11] Furthermore, it has been reported that head-to-tail-linked polythiophene moieties having phenoxy radical side chains exhibit ferromagnetic interactions.[12,13] Recently, Swager et al. reported the preparation of 1,3-bisdiphenylene-2-phenylallyl-based π-conjugated radical polymers as magneto-optic materials that show intense Faraday rotations as a new strategy for the development and application of organic magnets.[14] Furthermore, spin arrangement by the macroscopic ordering of molecular aggregates has been reported.[15]

Accordingly, research into metal-based antiferromagnetic materials, paramagnetic materials, and topological magnets as alternatives to ferromagnetic materials in the development of high-performance magnetic devices has increased.

Liquid crystals (LCs) are self-organizing materials and cholesteric liquid crystals (CLCs) are chiral LCs that have helical structures. Our group has developed a method for electrochemical polymerization in LCs. Electrochemical polymerization in CLCs affords π-conjugated polymer films with CLC-like helical morphologies and optical activity owing to chirality transfer from the CLC.[16,17] This method allows the synthesis of chiral polymers from achiral monomers. Optically active chiral polymers with no stereogenic centers are obtained as atropisomers from achiral monomers via asymmetric electrochemical or chemical LC polymerization, as developed by our group.[18] Furthermore, the electrochemical behavior of polarons (radical cations) and bipolarons (dications) as charge carriers in helical π-stacking backbones has been evaluated.[19,20]

In the present study, the synthesis of a chiral π-conjugated polymer from an achiral monomer bearing a stable organic radical was performed using electrochemical polymerization in a CLC. Introduction of chiral substituents to the side chains of the conjugated polymer leads to chiroptical activity and the formation of chiral J-aggregates owing to π-stacking of the main chain.[21−23] Furthermore, electrochemical polymerization

Received: February 7, 2019
Revised: March 24, 2019

DOI: 10.1021/acs.macromol.9b00274
Macromolecules XXXX, XXX, XXX−XXX

Scheme 1. Synthetic Routes to the Monomers Employed in This Study[a]

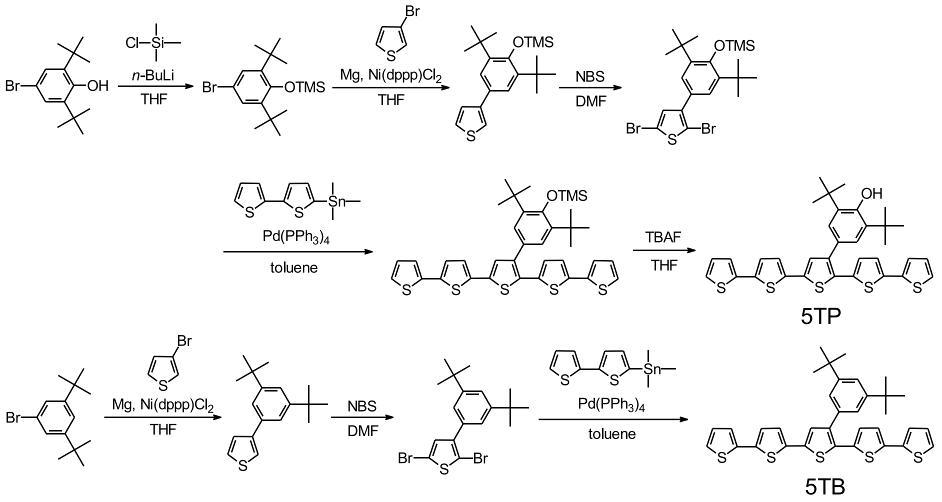

[a] n-BuLi: n-butyllithium, THF: tetrahydrofuran, Ni(dppp)Cl_2: dichloro[1,3-bis(diphenylphosphino)propane]nickel(II), NBS: n-bromosuccinimide, DMF: N,N-dimethylformamide, $Pd(PPh_3)_4$: tetrakis(triphenylphosphine)palladium(0), TBAF: tetrabutylammonium fluoride, TMS: trimethylsilyl group.

Table 1. Constituents of the Electrolyte CLC Solutions

Constituents	Chemical structure	wt%
Nematic LC	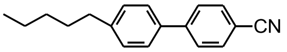 4-Cyano-4'-pentylbiphenyl (5CB)	95.0
Chiral inducer	Cholesteryl pelargonate (CP) 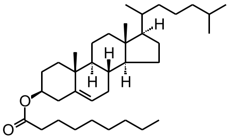 or (R)-8BpB6 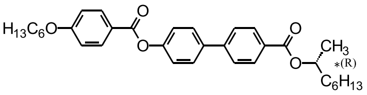	4.29
Supporting salt	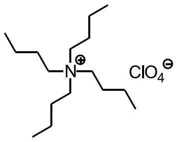 Tetrabutylammonium perchlorate (TBAP)	0.235
Monomers	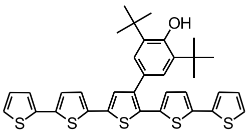 5TP or 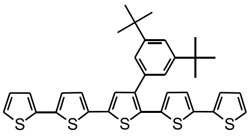 5TB	0.475

in CLCs requires no chiral modification of the monomer substituents. Thus, chiral polymers can be obtained from monomers with simple structures using polymerization in LC.

First, a thiophene pentamer bearing a 2,6-di-*tert*-butyl phenol side group as a precursor of the stable radical was synthesized. Next, optically active polymer films were prepared in a CLC. The resultant polymers show magneto-electro-optical activity.

The redox properties of the polymer films were investigated by optical and electrochemical analysis, and the magnetic properties of the polymer were investigated by superconducting quantum interference device (SQUID) magnetometry. The

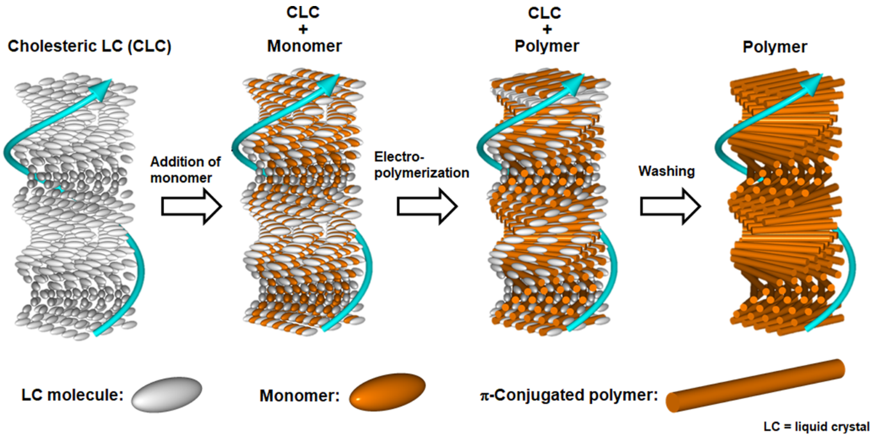

Figure 1. Possible process for electrochemical polymerization in a CLC medium showing the resultant transcription of its helical structure. White ellipsoids are CLC matrix molecules. Orange ellipsoids are monomers. Orange sticks are the resultant polymer.

Scheme 2. Synthetic Routes to p5TP$_{1\text{-radical}}$, p5TB$_{1\text{-red}}$, and p5TB$_{2\text{-red}}$.[a]

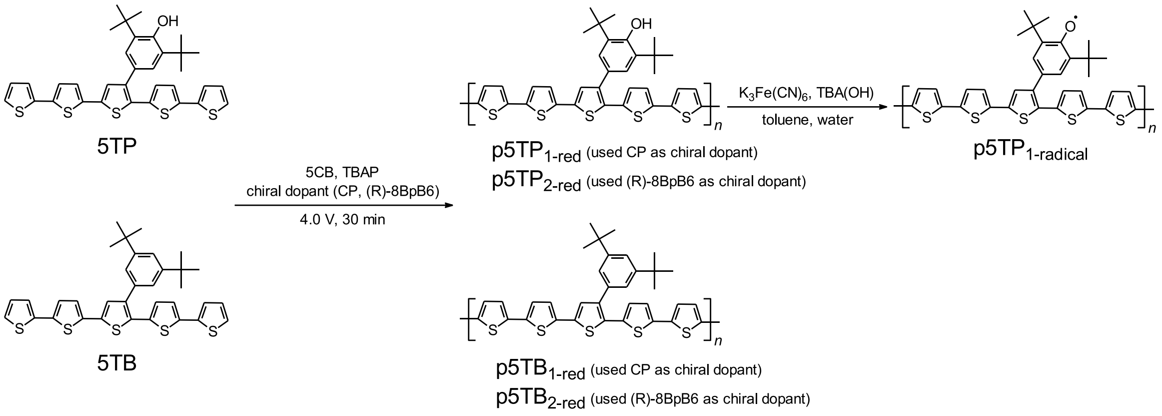

[a]Reduced (dedoped) polymers are obtained by treatment with hydrazine vapor. $K_3Fe(CN)_6$: potassium ferricyanide; TBA(OH): tetrabutylammonium hydroxide.

transfer of chirality from the CLC matrix to the phenoxy radicals in the side chain was confirmed. The circular dichroism (CD) absorption spectroscopy and the SQUID results indicated that the chiral magnetic polymers obtained in this study exhibit chiral helical spins with magneto-optical activity.

■ RESULTS AND DISCUSSION

Synthesis of Monomers. 3″-(3,5-Di-*tert*-butyl-4-phenoxy)-2,2′:5′,2″:5″,2‴:5‴,2⁗-quinquethiophene (5TP) and 3″-(3,5-di-*tert*-butyl-phenyl)-2,2′:5′,2″:5″,2‴:5‴,2⁗-quinquethiophene (5TB) were used as monomers for electrochemical polymerization in a CLC. The synthetic routes to the monomers are illustrated in Scheme 1. 5TP is a thiophene pentamer bearing a 2,6-di-*tert*-butyl phenol substituent as a side group and adopts a rodlike structure suitable for electrochemical polymerization in LCs. In addition, polymerization of a monomer having a bulky nonradical side group was also performed for comparison.[24] 5TB has a structure analogous to that of 5TP but without the phenoxy radical.[25] ^{1}H NMR and infrared (IR) absorption spectrometry were used for identification of the monomers (Figures S1−S9, Supporting Information, SI). In the IR spectrum of 5TP, the signal derived from the OH substituent is observed at 3618 cm^{-1} as a sharp peak due to the absence of hydrogen bonding, and the signal derived from the methyl substituent is observed at 2956 cm^{-1}. As expected, 5TB shows no signal for OH stretching. Thus, the IR data confirm the successful syntheses of 5TP and 5TB.

Polymer Synthesis. 4-Cyano-4′-pentylbiphenyl (5CB), which is a nematic LC at room temperature, was used as an achiral LC matrix (i.e., the host LC). The addition of chiral compounds to such matrices produces CLCs, which are chiral versions of nematic LCs. Cholesteryl pelargonate (CP) is used as a chiral dopant to induce a helical structure, and the previously synthesized (*R*)-4′-(4-hexyloxybenzoyloxy)-biphenyl-4-carboxylic acid 1-methylheptyl ester ((*R*)-8BpB6) is used as a chiral dopant to induce the corresponding opposite-handed helical structure. We performed electrochemical polymerization in the CLC. The constituents of the electrolytic CLC solution for electrochemical polymerization of 5TP and 5TB are summarized in Table 1. The electrolytic CLC solution was prepared by adding the monomer (5TP or 5TB) and tetrabutylammonium perchlorate (TBAP) as a supporting salt to the CLC solution. This electrolytic CLC solution was injected between two indium−tin oxide (ITO) coated glass electrodes as an anode and a cathode separated by a poly(tetrafluoroethylene) spacer of 200 μm thickness.

First, the polymerization cell is heated to form an isotropic electrolyte solution. The cell is then cooled and kept at room temperature to allow the formation of the CLC phase. In the polymerization cell, the helical axes of the CLC are arranged

DOI: 10.1021/acs.macromol.9b00274

parallel to the substrate electrodes to form fingerprint textures. Then, a direct current of 4.0 V is applied across the ITO electrodes and the polymerization reaction is performed for 30 min. After polymerization, the remaining CLC solution is removed by washing with *n*-hexane, affording the desired polymeric thin film on the anodic surface.

Figure 1 illustrates the CLC polymerization process. First, the monomer molecules align between the interhelical directors. Then, the polymer grows along the direction of the CLC, forming a helical aggregation structure. Simultaneously, phase separation between the matrix CLC and the resultant polymer occurs. Finally, washing with an organic solvent yields the helical polymer as the final product. In this case, the CLC matrix functions as a helical guide for polymerization. The reduced (dedoped) polymer can be subsequently obtained by exposure to hydrazine vapor, yielding $p5TP_{1\text{-red}}$ and $p5TB_{1\text{-red}}$ used CP as the chiral dopant and $p5TP_{2\text{-red}}$ and $p5TB_{2\text{-red}}$ used (*R*)-8BpB6 as the different type of chiral dopant (Scheme 2). The polymers contain no matrix LC fractions due to phase separation between the resultant polymer and the matrix LC during electrochemical polymerization.

The surface structures of the resultant polymeric thin films were observed using circular polarized differential interference contrast optical microscopy (C-DIM). The polymer exhibits a fingerprint-like texture with labyrinth-like stripes, indicating the transcription of the helical continuum of the CLC to the polymer (Figure 2). CD and ultraviolet–visible (UV–vis) optical absorption spectroscopy measurements of the polymer films reduced by hydrazine vapor confirm the transcription of the helical structure to the polymer. For the reduced (dedoped) polymers $p5TP_{1\text{-red}}$ and $p5TB_{1\text{-red}}$, a negative signal is observed at long wavelengths and a positive signal is observed at short wavelengths in the CD (Figure S10, Supporting Information, SI). In the case of the reduced polymers $p5TP_{2\text{-red}}$ and $p5TB_{2\text{-red}}$, a positive signal is observed at long wavelengths and a negative signal is observed at short wavelengths in the CD (Figure S11, Supporting Information, SI). Therefore, p5TP and p5TB with opposite helical structures are synthesized using CP and (*R*)-8BpB6 as chiral dopants that induce corresponding opposite helical structures. The inflection point of the CD is located at the maximum wavelength of the UV–vis absorption spectrum. The agreement between the CD and the UV–vis results indicates that the main chain forms a helical π-stacking structure. The linear dichroism spectra have very small value and are negligible compared to the CD signals.

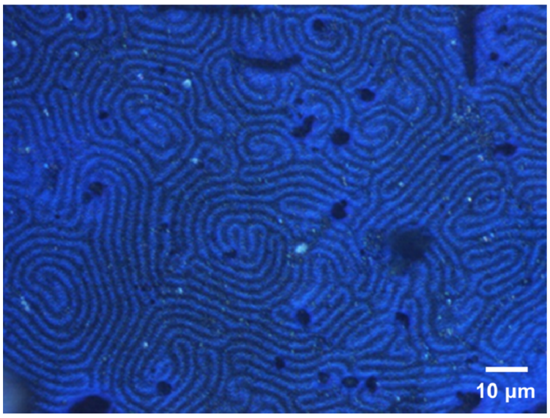

Figure 2. Circular polarized differential interference contrast optical microscopy (C-DIM) image of the surface structure of a polymer film at room temperature.

Electrochemical Properties of the Polymer Films. The electrochemical properties of the polymer films are investigated using cyclic voltammetry (CV), as shown in Figure 3. The CV measurements are carried out in a monomer-free 0.1 M TBAP–acetonitrile solution at the scan rates of 10–500 mV s^{-1}. The potentials are measured relative to a silver–silver ion (Ag/Ag^+) reference electrode. During the oxidation (doping) process for the $p5TP_1$ film, an oxidation signal at 0.596 V (scan rate: 10 mV s^{-1}) is observed, and the potential of the oxidation signal gradually increases with scan rate. The oxidation signal is shifted to 0.847 V at a scan rate of 500 mV s^{-1}. During the reduction (dedoping) process for the $p5TP_1$ film, a reduction signal at 0.517 V (scan rate: 10 mV s^{-1}) is observed, and the potential of the reduction signal is largely constant up to 500 mV s^{-1}.

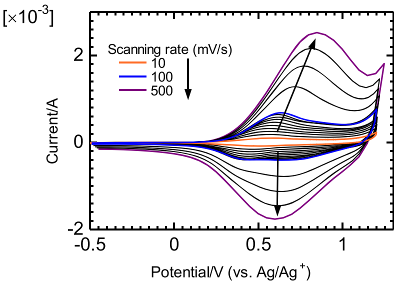

Figure 3. CV results for a $p5TP_1$ film on ITO glass using 0.1 M TBAP–acetonitrile solution at the scan rates of 10, 20, 30, 40, 50, 60, 70, 80, 90, 100, 200, 300, 400, and 500 mV s^{-1}.

In addition, the redox properties of the $p5TP_1$ film are evaluated by plotting the intensity of the signal for each scan rate (Figure S12, Supporting Information, SI). In the oxidation and reduction processes, the $p5TP_1$ film exhibits good redox properties, since the intensity change of the signal is linear. Similar electrochemical properties are observed for the $p5TB_1$ film (Figure S13, Supporting Information, SI), indicating that both these polymers are electroactive.

The in situ optical absorption spectra for the $p5TP_1$ film are obtained at various voltages in monomer-free 0.1 M TBAP–acetonitrile solution (Figure 4). Absorption bands at 488 nm (derived from π–π^* transition of the main chain), 777 nm (due to polarons (radical cations) of the doping band), and >1000 nm (due to bipolarons (dications) of the doping band) are observed (Figure 4a). Electrochemical redox processes change these absorption bands. The band at 488 nm decreases in intensity with increasing voltage, and the polaron and bipolaron bands appear at longer wavelengths. The absorption band at 488 nm increases and the doping bands decrease for the reduction process. The reduction process is equivalent to electrochemical dedoping. Furthermore, this electrochemical doping–dedoping is repeatable. The color of the $p5TP_1$ film changes from red (reduced state) to black (oxidized state) during the electrochemical processes.

The in situ CD optical absorption of the $p5TP_1$ film is also examined during the electrochemical redox process (Figure 4b). A negative signal at 571 nm and a positive signal at 438 nm are observed for the reduced state at 0 V, and the inflection point of the spectral change in the oxidation (doping) process

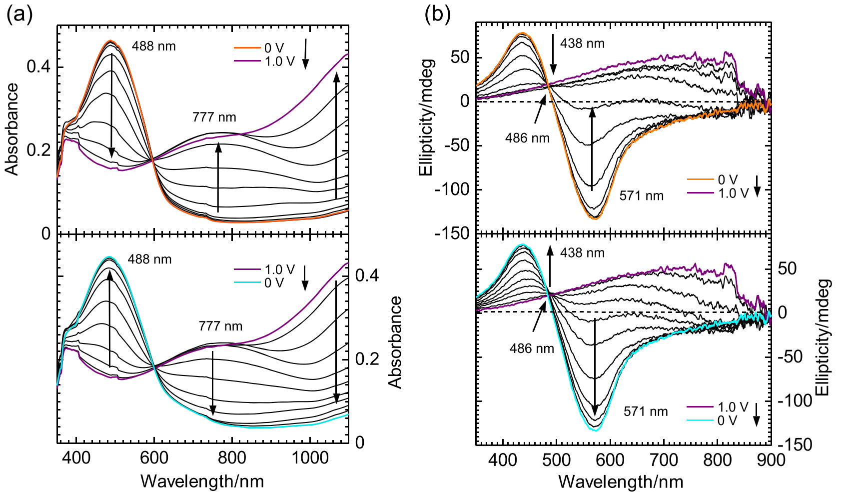

Figure 4. In situ optical absorption spectra for a p5TP$_1$ film in 0.1 M TBAP−acetonitrile solution at different voltages. (a) UV−vis optical absorption spectra, and (b) CD spectra of a p5TP$_1$ film during oxidation (upper) and reduction (bottom) between 1.0 and 0 V at 0.1 V steps.

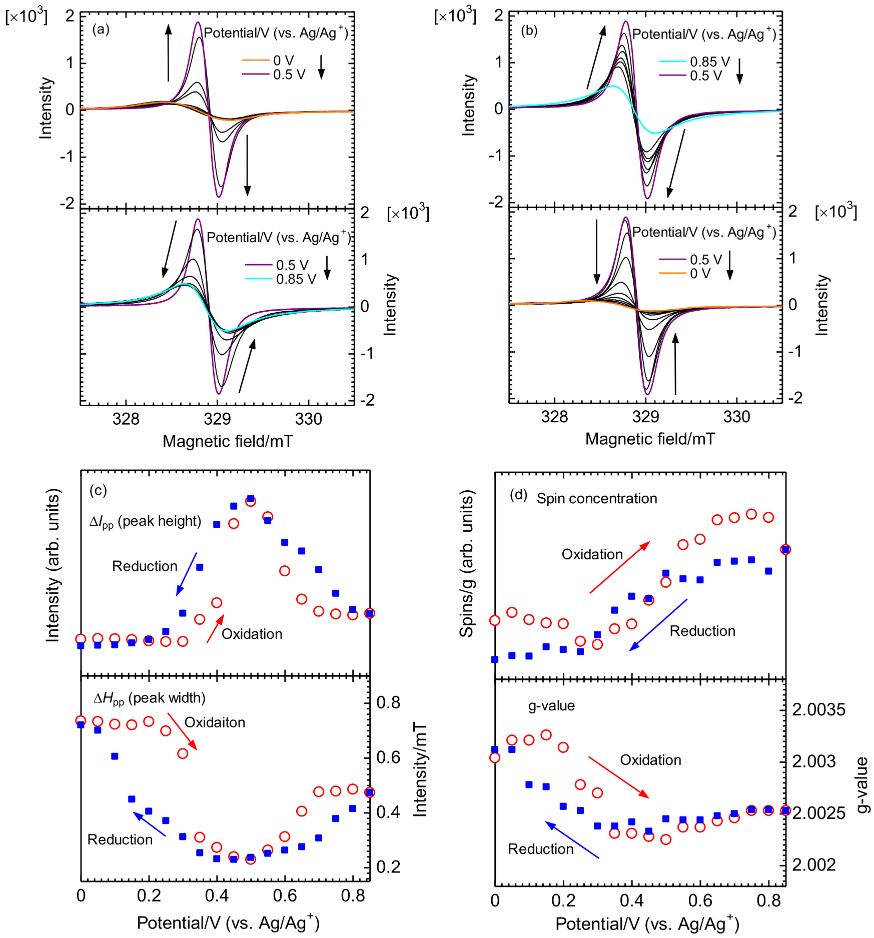

Figure 5. ESR data for a p5TP$_1$ film during electrochemical oxidation (a) and reduction (b) vs Ag/Ag$^+$ at 0.05 V steps. (c) Peak height (ΔI_{pp}) and peak width (ΔH_{pp}). (d) The g-value and spin concentration.

is observed at 486 nm. The p5TP$_1$ film exhibits a Cotton effect associated with the π−π* transition of the main chain. This is reversible in the redox process (i.e., electrochemical doping−dedoping). In addition, this repeatable inversion of the Cotton effect at 486 nm upon changes in the electrochemical state of the polymer indicates that the polymer has a one-handed chiral structure and that the chirality can be tuned by changing the electronic state of the main chain by doping. Similar redox-driven optical behavior is observed for the p5TB$_1$ film, indicating that the polymer is electro-optically active (Figure S14, Supporting Information, SI).

The electrochemical properties of p5TP$_2$ and p5TB$_2$ synthesized using (R)-8BpB6, which is a different type chiral dopant, are similarly measured by using optical absorption and

CD spectroscopy measurements (Figure S15, Supporting Information, SI). The UV−vis absorption spectra by electrochemical redox process show the same behavior as $p5TP_1$ and $p5TB_1$. However, the CD of $p5TP_1$ with electrochemical redox process shows opposite behavior to that of $p5TB_1$, indicating the formation of $p5TP_2$ and $p5TB_2$ having opposite helical structures using (*R*)-8BpB6, which is a chiral dopant different from CP.

Electron-Spin Resonance (ESR) Analysis. The generation of polarons and bipolarons by the $p5TP_1$ film is confirmed using in situ optical absorption spectra recorded during electrochemical processes at different voltages. In the polaron state, radical, and cation pairs are generated along the *π*-conjugated polymer backbone. The ESR spectra for the $p5TP_1$ film on an ITO glass substrate are measured at different voltages. In the oxidation process (Figure 5a), the intensity of the ESR signal increases from 0 to 0.5 V with the generation of polarons and then gradually decreases with the generation of bipolarons (dications) from 0.5 to 0.85 V. This behavior occurs reversibly in the reduction process (Figure 5b). Figure 5c,d shows the plots of ESR line widths (ΔH_{pp}), *g*-values, peak heights (ΔI_{pp}), and spin concentrations at different voltages. A decrease in ΔH_{pp} is observed with the generation of polarons up to 0.5 V. Further voltage increase leads to an increase in ΔH_{pp} with the generation of bipolarons. The spin concentration also increases with the generation of polarons in the main chain. In addition, the increase of polarons in the main chain between 0.25 and 0.35 V decreases the *g*-value. Further application of voltage (>0.4 V) for the polymer results in a constant *g*-value (2.0025). The *g*-value of 2.0025 for the polymer confirms the formation of polarons as charge carriers in the main chain. The ESR results are consistent with the UV−vis absorption spectra, which reveal the generation of the polaron band at 777 nm with increasing voltage. The CD results are also consistent with the ESR results. For the $p5TB_1$ film, the *g*-value is constant at 2.0025 due to the formation of polarons, and the spin concentration increases with electrochemical doping (i.e., increase of voltage), as shown in Figure S16, Supporting Information (SI).

Chirality of the Phenoxy Radical Side Groups. The phenoxy radical side group could potentially exists in a chiral environment because the main chain of the polymer exhibits one-handed chirality endowed by chirality transcription upon electrochemical polymerization in a CLC. Accordingly, we performed electrochemical oxidation to generate radicals at the oxygen atoms of the $p5TP_1$ side groups. CV measurements were performed in 0.1 M TBAP and a small amount of tetrabutylammonium hydroxide (TBA(OH)) in acetonitrile at a scan rate of 10 mV s^{-1} (Figure 6). In the oxidation process, an oxidation signal derived from the generation of phenoxy radicals is observed at −0.110 V. This potential is different from that of the signals derived from the polarons in the main chain. A previous study reported that the oxidation potential of the phenoxy radical in the side chain of polythiophene is −0.10 V. This value is in good agreement with that in this study.[13] Selective electrochemical oxidation and generation of phenoxy radicals is possible because the oxidation potential for the generation of phenoxy radicals in the side groups is independent of the generation of polarons in the main chain. Furthermore, optical measurements confirmed the generation of phenoxy radicals in the polymer upon application of different potentials. Figure 7a shows the CD traces for the polymer at −0.2 V (before the generation of phenoxy radicals) and 0.1 V (after the generation of phenoxy radicals). Figure 7c displays the optical absorption spectra of the polymer before and after the generation of polarons. The polymer exhibits CD signals owing to its one-handed helical structure. The sign of the split-type CD signals changes from negative to positive (negative first and then positive at long wavelengths) as a form of Davydov splitting, indicating that the main chain forms a left-handed helical structure (according to previous research by Berova and Nakanishi).[30] The generation of phenoxy radicals side groups causes a slight change in the CD and the UV−vis spectra. The CD signal of the spins overlaps with the entire absorption spectrum due to the helical structure of the main chain. Difference spectrum can extract the CD signal of the magnetic spins. Figure 7b,d shows the difference spectra for before and after the generation of phenoxy radicals. Optical absorption due to the phenoxy radicals is observed at 532 nm, which is in good agreement with the results of a previous study.[13] In the CD spectra, the peak of the negative signal is observed at around 600 nm and that of the positive signal at around 440 nm. Note that the phenoxy radical for $p5TP_1$ exhibits a Cotton effect, indicating that the phenoxy radicals possess chirality due to the twist of the main chain, which is produced by the CLC transcription polymerization. Thus, the radicals form helical structures based on the helical chirality of the main chain. In other words, a helical spin state is realized through the one-handed helical arrangement of the organic polymer. The split-type difference spectrum shows changes in the CD sign with wavelength, indicating that the radicals as chromophores form a left-handed helical structure. $p5TB_1$ shows a different tendency than $p5TP_1$ in the CD results (Figure S17, Supporting Information, SI). No spectral changes due to the absence of phenoxy radical are observed in this potential range. These results strongly indicate that the application of potentials to $p5TP_1$ generates phenoxy radicals with left-handed helical spins.

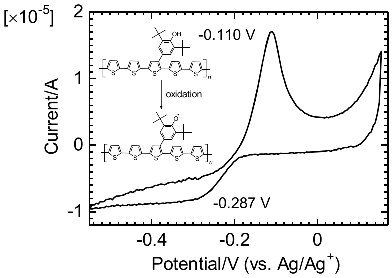

Figure 6. CV trace for a $p5TP_1$ film on an ITO glass substrate obtained using a 0.1 M TBAP/TBA(OH)/acetonitrile solution at a scan rate of 10 mV s^{-1}.

Magnetic Properties of the Polymer. The different oxidation potentials for the generation of phenoxy radicals and polarons in the polymer allow the selective chemical oxidation of OH to generate phenoxy radicals in the side groups. A previous study reported the selective generation of phenoxy radicals using $K_3Fe(CN)_6$ as an oxidizing agent.[13] Thus, we performed selective chemical oxidation for the present polymers. First, a small amount of TBA(OH) was added to $p5TP_{1\text{-red}}$ in toluene (2 mL) and the solution was stirred for 6 h under a nitrogen atmosphere. Then, $K_3Fe(CN)_6$ (0.2 g) in water (1 mL) was added to this solution and stirred for 2 h at room temperature. The resultant compound was washed with water three times and dried under reduced pressure to give the desired product ($p5TP_{1\text{-radical}}$) bearing phenoxy radicals

DOI: 10.1021/acs.macromol.9b00274
Macromolecules XXXX, XXX, XXX−XXX

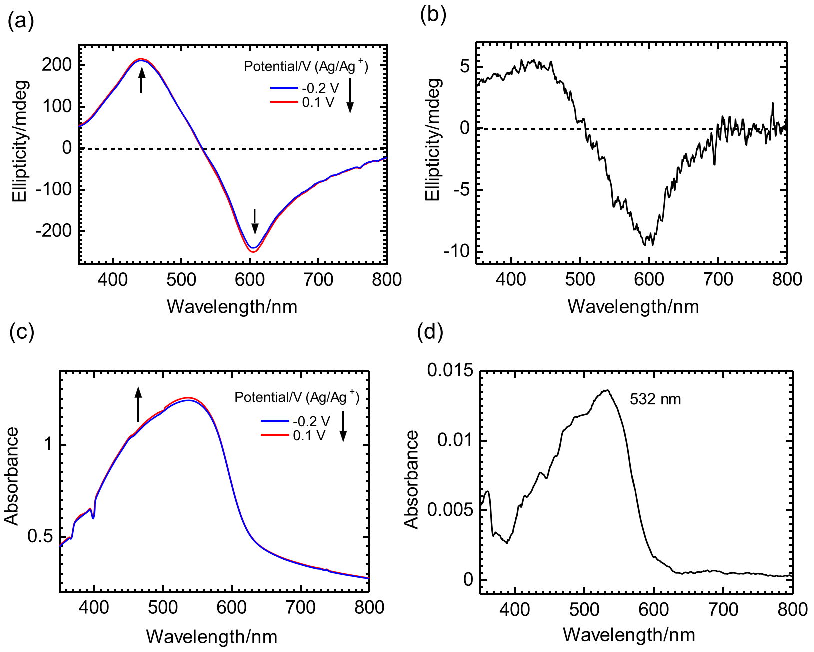

Figure 7. In situ CD spectra (a) and UV−vis absorption spectra (c) for a p5TP$_1$ film at −0.2 V (before the generation of phenoxy radicals) and 0.1 V (after the generation of phenoxy radicals) in 0.1 M TBAP and TBA(OH) in acetonitrile. (b) CD difference spectrum. (d) UV−vis difference spectrum.

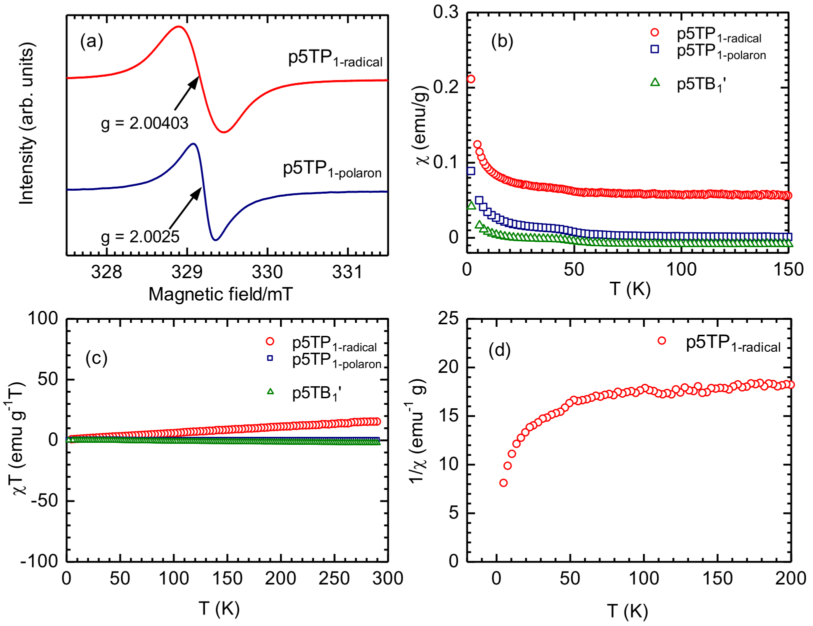

Figure 8. (a) ESR spectra for p5TP$_{1\text{-radical}}$ (red line) and p5TP$_{1\text{-polaron}}$ (blue line). (b) χ vs T plots for p5TP$_{1\text{-radical}}$, p5TP$_{1\text{-polaron}}$, and p5TB$_1'$. (c) χT vs T plots for the polymers (Curie−Weiss plot, $C = \chi T$). (d) $1/\chi$ vs T for p5TP$_{1\text{-radical}}$. χ: Magnetic susceptibility.

(Scheme 2). As a control, p5TP$_{1\text{-polaron}}$ in the polaron state, synthesized by electrochemical polymerization in a CLC, was examined for comparison. Radical species were identified for p5TP$_{1\text{-radical}}$ by ESR measurements (Figure 8a). In the ESR spectrum of p5TP$_{1\text{-radical}}$, the g-value of the phenoxy radical is 2.00403, whereas that of the polarons in p5TP$_{1\text{-polaron}}$ is 2.0025, indicating that the radical species in p5TP$_{1\text{-polaron}}$ are not phenoxy radicals. In addition, the spin concentration of p5TP$_{1\text{-radical}}$ is 1.53×10^{19} spin g^{-1}, which is higher than that of p5TP$_{1\text{-polaron}}$ (Table 2). p5TB$_1'$ as a control polymer for comparison with p5TB$_{1\text{-red}}$ was synthesized using the same method as that for p5TP$_{1\text{-radical}}$. No ESR signals for p5TB$_1'$ are detected, indicating that the oxidizing agent (K$_3$Fe(CN)$_6$) generates no polarons as charge carriers in the main chain. This result demonstrates that K$_3$Fe(CN)$_6$ can be used to

Table 2. ESR Results for p5TP$_{1\text{-radical}}$, p5TP$_{1\text{-polaron}}$, and p5TB$_1'$

	ΔH_{pp} (mT)	g-value	spin conc. (spins g^{-1})
p5TP$_{1\text{-radical}}$	0.569	2.00403	1.53×10^{19}
p5TP$_{1\text{-polaron}}$	0.286	2.00250	0.355×10^{19}
p5TB$_1'$	not detected		

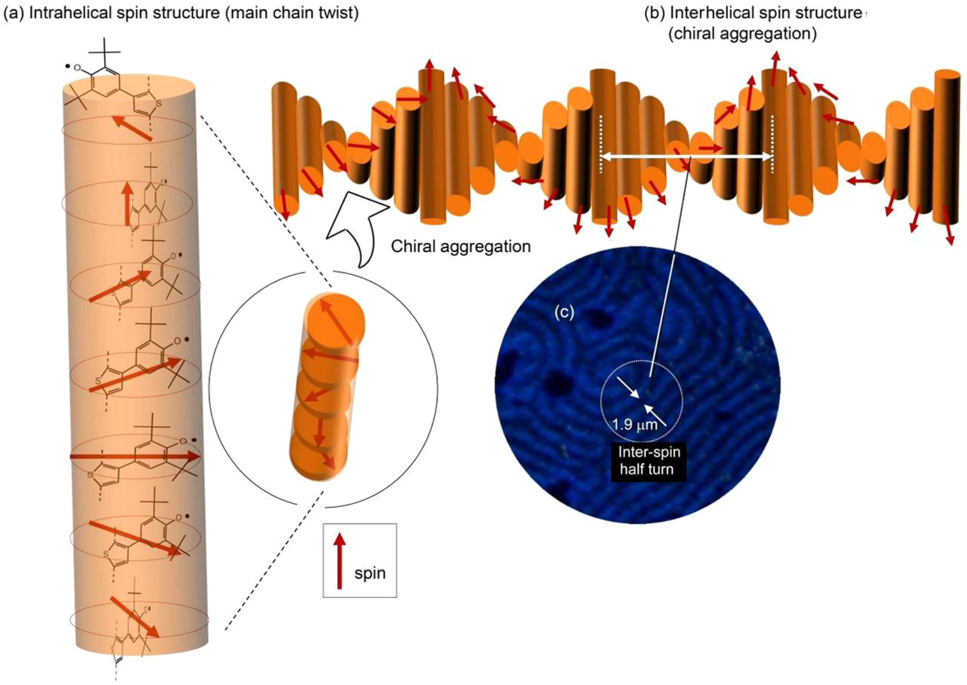

Figure 9. Plausible helical structure of the polymer. (a) Intrahelical spin structure of the polymer. (b) Interhelical spin structure produced by LC imprinting. (c) C-DIM image of the polymer showing helical stripes. The distance between the stripes of the optical structure corresponds to the helical half-pitch.

generate phenoxy radicals on the side groups without generating polarons in the main chain.

The magnetic susceptibility of the polymers was measured using SQUID magnetometry, as shown in Figures 8b. p5TP$_{1\text{-radical}}$ exhibits intense magnetic susceptibility compared to p5TP$_{1\text{-polaron}}$ and p5TB$_1'$. The residual oxygen in the samples presents weak signals at around 40 K. Figure 8c shows the χT vs T (i.e., Curie−Weiss plots) for the polymers. $1/\chi$ plotted as a function of temperature indicates the paramagnetism of p5TP$_{1\text{-radical}}$ (Figure 8d). The χT curve of p5TP$_{1\text{-radical}}$ slightly increases from low to high temperature owing due to interspin interactions dominating thermal vibrations at low temperature, although no clear inflection point at low temperature as antiferromagnetic behavior appeared.

p5TP$_{1\text{-radical}}$ exhibits intense magnetic susceptibility compared to p5TP$_{1\text{-polaron}}$ and p5TB$_1'$. The χT values for p5TP$_{1\text{-polaron}}$ are constant with temperature because the paramagnetic character of a small portion of polarons overlaps with the diamagnetism as the major magnetic behavior of the polymer, which is based on sp^2- and sp^3-hybridized chemical bonding, as shown in Figure 8c. p5TB$_1'$, which contains neither polarons nor phenoxy radicals, shows negative magnetism (i.e., diamagnetic behavior), as shown in Figure 8c (green triangles). Helical magnets can show paramagnetism or antiferromagnetism.[31] The CD results indicate that the magnetic spins in p5TP$_{1\text{-radical}}$ rotate to form an anticlockwise helix, and the SQUID results demonstrate that the polymer is magnetically active.

Furthermore, the LC matrix forms intermolecular anticlockwise helical aggregates, confirmed through miscibility test for the LC electrolyte solution. Cholesteryl oleyl carbonate with an anticlockwise helical architecture was employed as a standard cholesteric LC for determining the helical direction of the LC electrolyte solution containing monomer. No boundary was observed between the LC electrolyte solution region and the cholesteryl oleyl carbonate region on a glass cell, indicating the LC electrolyte solution forms an anticlockwise (left handed) helical structure. This demonstrates that the resultant LC-imprinted polymer forms a left-handed helix.

The p5TP$_{1\text{-radical}}$ thus obtained from the chiral LC forms π-stacking with an anticlockwise rotation to form a left-handed chiral aggregate as a result of imprinting by the LC matrix during polymerization. Thus, we conclude that the CD and SQUID results confirm that p5TP$_{1\text{-radical}}$ exhibits a main chain anticlockwise helical spin order and an anticlockwise helical aggregation of the main chains. In other words, p5TP$_{1\text{-radical}}$ with magneto-optical activity comes from the hierarchical intramolecular helical spin order and the CLC-like intermolecular three-dimensional (3D) helical structure. The M−H curve (magnetization curve) of the polymer shows no hysteresis loop, confirming this polymer is a paramagnetic material. The helical structure is stabilized by intermolecular π-stacking, resulting in a solid polymer film that exhibits magnetism.

Plausible Structure. Figure 9 shows a plausible structure for the polymer prepared in a CLC. The main chain of the polymer thus prepared in the twisted reaction field of the chiral LC forms a twisted helical structure. This main chain forms an intrahelical spin structure accompanied by helical twisting of the main chain, as shown in Figure 9a. In Figure 9b, the cylinder form represents an individual main chain. The main chains undergo one-handed 3D helical aggregation upon the LC imprinting reaction, as shown in Figure 9c. The helical spins in the main chain form an interhelical structure. The distance between the helical stripes of the fingerprint texture corresponds to the helical half-pitch (1.9 μm). Therefore, one rotation of the helical spin is 3.8 μm, which is accompanied by the helical twist of the aggregated structure. The polymer shows no ferromagnetic spin alignment because the polymer thus synthesized in this study satisfies none of the conditions of topological spin parallel alignment required to obtain ferromagnetic order.[32,33] The polymer forms a one-handed chiral continuum from the molecular level to that of macroscopic chiral aggregation with hierarchical intrahelical and interhelical spin orders.

CLCs form a quasi-layered structure similar to the smectic state observed for the formation of fan-shaped textures.[34] The polymer prepared in the CLC exhibits a similar pattern of helical magnetic domains to that observed for inorganic magnets.[35] Although the CLC forms no crystal-like domain structures, p5TP$_{1\text{-radical}}$ exhibits a magnetic-domain-like structure produced by imprinting in the CLC.

■ CONCLUSIONS

Organic polymers generally form amorphous solids having partly crystalline regions. LC polymers have crystal-like molecular order. However, conjugated LC polymers with side groups require the addition of a bulky mesogen (an LC generator) to the skeleton, resulting in the depression of electronic performance. Polymerization in LC avoids this drawback because the resultant polymers form LC structures via imprinting from the matrix LC without the need for a mesogen in the polymer. The LC transcription method we propose here allows further chirality imprinting from the LC matrix to the resultant polymer. The combination of π-stacking and the rigid form of the conjugated main chain, its chirality, and the stable spin state in the side group affords magneto-electro-optically active polymers. The spin chirality of the polymer is derived from the intramain chain and the intermain chain helicity. Helical spins have been directly observed previously for $Fe_{0.5}Co_{0.5}Si$ as an inorganic magnet with Lorentz electron microscopy.[35] In the case of the polymer synthesized in this study, optical microscopy conveniently reveals the spin helical order of the paramagnetism through the observation of the LC-like texture of the polymer. This is the first example of an optically active helical spins constructed from an organic polymer.

■ EXPERIMENTAL SECTION

Synthesis of (2,6-Di-*tert*-butyl-4-bromophenoxy)-trimethylsilane. This synthesis was carried out according to a previously reported method.[26] Quantities used: 2,6-di-*tert*-butyl-4-bromophenol (5.01 g, 17.6 mmol), *n*-butyllithium (16.5 mL, 26.3 mmol, 1.6 M in hexane), chlorotrimethylsilane (3.55 g, 32.7 mmol), and THF (70 mL). Yield = 92% (5.77 g, 16.1 mmol). ^{1}H NMR (400 MHz; $CDCl_3$; δ from TMS, ppm), 0.418 (s, 9H), 1.394 (s, 18H), 7.324 (s, 2H).

Synthesis of 3-(3,5-Di-*tert*-butyl-4-trimethylsiloxyphenyl)-thiophene. This synthesis was carried out according to a previously reported method.[27,28] Quantities used: Mg (0.31 g, 12.8 mmol), (2,6-di-*tert*-butyl-4-bromophenoxy)trimethylsilane (3.50 g, 9.8 mmol), 3-bromothiophene (1.95 g, 11.9 mmol), [1,3-bis(diphenylphosphino)-propane]nickel(II) chloride ($NiCl_2$(dppp), 0.044 g, 0.081 mmol), and THF (30 mL). Yield = 45% (2.07 g, 5.75 mmol). ^{1}H NMR (400 MHz; $CDCl_3$; δ from TMS, ppm), 0.453 (s, 9H), 1.47 (s, 18H), 7.36 (m, 3H), 7.493 (s, 2H).

Synthesis of 2,5-Dibromo-3-(3,5-di-*tert*-butyl-4-trimethylsiloxyphenyl)thiophene. This synthesis was carried out according to a previously reported method.[27,28] Quantities used: 3-(3,5-di-*tert*-butyl-4-trimethylsiloxyphenyl)thiophene (2.73 g, 7.58 mmol), *n*-bromosuccinimide (NBS, 2.97 g, 16.68 mmol), and DMF (50 mL). Yield = 38% (1.51 g, 2.91 mmol). ^{1}H NMR (400 MHz; $CDCl_3$; δ from TMS, ppm), 0.511 (s, 9H), 1.511 (s, 18H), 7.099 (m, 1H), 7.49 (s, 2H).

Synthesis of 5-Trimethyltin-2,2′-bithiophene. This synthesis was carried out according to a previously reported method.[29] Quantities used: bithiophene (4.5 g, 27.07 mmol), *n*-butyllithium (17 mL, 27.07 mmol), trimethyltin chloride (5.39 g, 27.07 mmol), and THF (50 mL). The crude product was used in the next step without purification.

Synthesis of 3″-(3,5-Di-*tert*-butyl-4-trimethylsiloxyphenyl)-2,2′:5′,2″:5″,2‴:5‴,2⁗-quinquethiophene. Under argon atmosphere, 2,5-dibromo-3-(3,5-di-*tert*-butyl-4-trimethylsiloxyphenyl)-thiophene (162 mg, 0.313 mmol) and 5-trimethyltin-2,2′-bithiophene (226 mg, 0.688 mmol) in toluene (3 mL) were added to an overdried 50 mL round-bottom flask equipped with a stir bar and stirred for 0.5 h. Then, tetrakis(triphenylphosphine)palladium(0) (7.23 mg, 0.00626 mmol) was added to this solution and stirred under reflux at 75 °C for 24 h. After that, the reaction mixture was poured into water and extracted with ethyl acetate. The organic layer was washed with water and dried over $MgSO_4$. The solvent was evaporated. The product was purified by column chromatography (silica gel, eluent: hexane) to afford the desired product (22 mg, 0.0319 mmol, yield: 10%). ^{1}H NMR (400 MHz; $CDCl_3$; δ from TMS, ppm), 0.454 (s, 9H), 1.407 (s, 18H), 6.944 (d, 1H, $J = 4.0$ Hz), 6.973 (dd, 1H, $J = 1.6$ Hz), 6.996 (d, 1H, $J = 4.0$ Hz), 7.036 (m, 2H), 7.116 (dd, 2H, $J = 3.33$ Hz), 7.163 (s, 1H), 7.187 (m, 2H), 7.235 (dd, 1H, $J = 1.87$ Hz), 7.301 (s, 2H).

Synthesis of 3″-(3,5-Di-*tert*-butyl-4-phenoxy)-2,2′:5′,2″:5″,2‴:5‴,2⁗-quinquethiophene (5TP). Under argon atmosphere, 3″-(3,5-di-*tert*-butyl-4-trimethylsiloxyphenyl)-2,2′:5′,2″:5″,2‴:5‴,2⁗-quinquethiophene (22 mg, 0.0319 mmol) and tetrabutylammonium fluoride (1 M in THF, 0.1 mL, 0.1 mmol) in THF (3 mL) were added to an overdried 50 mL round-bottom flask equipped with a stir bar and stirred for 4 h at room temperature. After that, the reaction mixture was poured into water and extracted with ethyl acetate. The organic layer was washed with water and dried over $MgSO_4$. The solvent was evaporated. The product was purified by column chromatography (silica gel, eluent: hexane) to afford the desired product (15.7 mg, 0.0255 mmol, yield: 80%). ^{1}H NMR (400 MHz; $CDCl_3$; δ from TMS, ppm), 1.445 (s, 18H), 5.304 (s, 1H), 6.952 (d, 1H, $J = 3.6$ Hz), 6.989 (dd, 1H, $J = 2.9$ Hz), 7.006 (d, 1H, $J = 4$ Hz), 7.037 (dd, 1H, $J = 2.9$ Hz), 7.061 (dd, 1H, $J = 1.5$ Hz), 7.116 (dd, 2H, $J = 3.1$ Hz), 7.144 (s, 1H), 7.192 (m, 2H), 7.236 (m, 1H), 7.242 (s, 2H). ^{13}C NMR ($CDCl_3$; δ from TMS, ppm), 30.4, 34.5, 123.4, 123.5, 123.8, 124.4, 124.5, 124.6, 126.2, 126.4, 126.8, 127.1, 127.9, 128.0, 135.1, 135.2, 135.9, 137.1. MALDI-TOF MS (m/z): $[M + 2H]^+$ calcd for $C_{34}H_{34}OS_5$, 618.1213; found, 618.1201. Mp 196.6 °C.

Synthesis of 3-(3,5-Di-*tert*-butyl-phenyl)thiophene. Under argon atmosphere, Mg (0.542 g, 22.3 mmol) in THF (5 mL) was added to an overdried 100 mL round-bottom flask equipped with a stir bar. Then, this solution was slowly added dropwise to 1-bromo-3,5-di-*tert*-butyl-benzene (5.00 g, 18.6 mmol) in THF (5 mL) and stirred for 6 h at room temperature. After the disappearance of Mg, this Grignard suspension was added to a mixture of 3-bromothiophene (3.03 g, 18.6 mmol) and [1,3-bis-(diphenylphosphino)propane]nickel(II) chloride ($NiCl_2$(dppp), 0.065 g, 0.120 mmol) in THF (10 mL) and stirred under reflux for 12 h. When the reaction is completed, the reaction mixture poured into an aqueous sodium bicarbonate ($NaHCO_3$) and extracted with ethyl acetate. The organic layer was washed with water and dried over $MgSO_4$. The solvent was evaporated. The product was purified by column chromatography (silica gel, eluent: hexane) to afford the desired product (3.54 g, 13.0 mmol, yield: 70%). ^{1}H NMR (400 MHz; $CDCl_3$; δ from TMS), 1.409 (s, 18H), 7.394−7.433 (m, 3H, 2,4,5-(thiophene)), 7.449−7.467 (m, 3H, 2,4,6-(benzene)).

Synthesis of 2,5-Dibromo-3-(3,5-di-*tert*-butyl-phenyl)-thiophene. Under argon atmosphere, 3-(3,5-di-*tert*-butyl-phenyl)-thiophene (3.50 g, 12.9 mmol) in DMF (15 mL) was added to an overdried 100 mL round-bottom flask equipped with a stir bar. After that, NBS (5.71 g, 32.1 mmol) was slowly added to the solution at 0

°C and stirred 24 h at room temperature. Then, the mixture was poured into an aqueous sodium bicarbonate ($NaHCO_3$) and extracted with ethyl acetate. The organic layer was washed with water and dried over $MgSO_4$. The solvent was evaporated. The product was purified by column chromatography (silica gel, eluent: hexane) to afford the desired product (3.58 g, 8.32 mmol, yield: 65%). ^{1}H NMR (400 MHz; $CDCl_3$; δ from TMS, ppm), 1.375 (s, 18H), 7.055 (s, 1H), 7.344 (d, 2H, J = 1.6 Hz), 7.434 (t, 1H, J = 1.8 Hz).

Synthesis of 3″-(3,5-Di-*tert*-butyl-phenyl)-2,2′:5′,2″:5″,2‴:5‴,2⁗-quinquethiophene (5TB). Under argon atmosphere, 2,5-dibromo-3-(3,5-di-*tert*-butyl-phenyl)thiophene (1.00 g, 2.32 mmol) and 5-trimethyltin-2,2′-bithiophene (1.68 g, 5.11 mmol) in toluene (10 mL) were added to an overdried 100 mL round-bottom flask equipped with a stir bar and stirred for 0.5 h. Then, tetrakis(triphenylphosphine)palladium(0) (53.0 mg, 0.0465 mmol) was added to this solution and stirred under reflux at 75 °C for 24 h. After that, the reaction mixture was poured into water and extracted with ethyl acetate. The organic layer was washed with water and dried over $MgSO_4$. The solvent was evaporated. The product was purified by column chromatography (silica gel, eluent: hexane) to afford the desired product (145 mg, 0.241 mmol, yield: 10%). ^{1}H NMR (400 MHz; $CDCl_3$; δ from TMS, ppm), 1.334 (s, 18H), 6.917 (d, 1H, J = 3.6 Hz), 6.982 (m, 2H), 7.041 (m, 2H), 7.122 (dd, 2H, J = 3.7 Hz), 7.166 (s, 1H), 7.192 (m, 2H), 7.237 (dd, 1H, J = 2.1 Hz), 7.278 (d, 2H, J = 2 Hz), 7.422 (t, 1H, J = 1.8 Hz). ^{13}C NMR ($CDCl_3$; δ from TMS, ppm), 31.5, 35.0, 121.6, 123.5, 123.6, 123.7, 123.8, 124.4, 124.5, 124.6, 126.9, 127.2, 127.9, 128.0, 134.7, 137.1, 137.2, 140.8, 150.9. MALDI-TOF MS (m/z): $[M + 2H]^+$ calcd for $C_{34}H_{34}S_5$, 602.1264; found, 602.1309. Mp 192.9 °C.

Instruments. Magnetic susceptibility measurements of the polymer were carried out using a superconductor interference devices (SQUID, Quantum Design CA, magnetic property measurement system, MPMS). ESR measurements were conducted using a JEOL (Tokyo) JES TE-200 spectrometer with 100 kHz modulation (X-band). ^{1}H NMR spectra were measured in $CDCl_3$ using a JEOLJNM-ECS-400 NMR spectrometer. Chemical shifts were recorded in parts per million downfield from tetramethylsilane (TMS) as an internal standard. Absorption spectra were obtained using a V-630 spectrometer (JASCO, Tokyo). Circular dichroism measurements were performed using a Jasco J-720 spectrometer. Electrochemical measurements of polymers were conducted using an electrochemical analyzer (μAutolab III, Autolab, the Netherlands), and optical textures were observed using a high-resolution polarizing microscope ECLIPS LV 100 with a Nikon LU Plan Fluor and Nikon CFIUW lenses without oil immersion (Nikon, Tokyo).

■ ASSOCIATED CONTENT

Ⓢ Supporting Information

The Supporting Information is available free of charge on the ACS Publications website at DOI: 10.1021/acs.macromol.9b00274.

> ^{1}H NMR data of the monomers; FT-IR spectra of the monomers; optical and electrochemical spectra of the polymer films; ESR spectra of the polymer films (PDF)

■ AUTHOR INFORMATION

Corresponding Author

*E-mail: gotoh@ims.tsukuba.ac.jp.

ORCID

Hiromasa Goto: 0000-0003-4276-735X

Notes

The authors declare no competing financial interest.

■ ACKNOWLEDGMENTS

We would like to thank the OPEN FACILITY, Research Facility Center for Science and Technology, University of Tsukuba, for using NMR, and Glass Work Shop of University of Tsukuba. This research was supported by KAKENHI (No. 17K05985).

■ REFERENCES

(1) Li, Z.; Ding, J.; Guo, C.; Lefebvre, J.; Malenfant, P. R. Decomposable s-tetrazine copolymer enables single-walled carbon nanotube thin film transistors and sensors with improved sensitivity. *Adv. Funct. Mater.* **2018**, *28*, No. 1705568.

(2) Guo, K.; Bai, J.; Jiang, Y.; Wang, Z.; Sui, Y.; Deng, Y.; Han, Y.; Tian, H.; Geng, Y. Diketopyrrolopyrrole-based conjugated polymers synthesized via direct arylation polycondensation for high mobility pure n-channel organic field-effect transistors. *Adv. Funct. Mater.* **2018**, *28*, No. 1801097.

(3) Hsiao, S. H.; Wang, H. M. Electrochemically fabricated electrochromic films from 4-(N-carbazolyl) triphenylamine and its dimethoxy derivative. *RSC. Adv* **2016**, *6*, 43470−43479.

(4) Jian, N.; Gu, H.; Zhang, S.; Liu, H.; Qu, K.; Chen, S.; Liu, X.; He, Y.; Niu, G.; Tai, S.; Wang, J.; Lu, B.; Xu, J.; Yu, Y. Synthesis and electrochromic performances of donor-acceptor-type polymers from chalcogenodiazolo [3,4-c] pyridine and alkyl ProDOTs. *Electrochim. Acta* **2018**, *266*, 263−275.

(5) Kan, B.; Zhang, J.; Liu, F.; Wan, X.; Li, C.; Ke, X.; Wang, Y.; Feng, H.; Zhang, Y.; Long, G.; Friend, R. H.; Bakulin, A. A.; Chen, Y. Fine-tuning the energy levels of a nonfullerene small-molecule acceptor to achieve a high short-circuit current and a power conversion efficiency over 12% in organic solar cells. *Adv. Mater.* **2018**, *30*, No. 1704904.

(6) Nishide, H.; Yoshioka, N.; Inagaki, K.; Kaku, T.; Tsuchida, E. Poly [(3,5-di-*tert*-butyl-4-hydroxyphenyl) acetylene] and its polyradical derivative. *Macromolecules* **1992**, *25*, 569−575.

(7) Yoshioka, N.; Nishide, H.; Kaneko, T.; Yoshiki, H.; Tsuchida, E. Poly [(*p*-ethynylphenyl) hydrogalvinoxy] and its polyradical derivative with high spin concentration. *Macromolecules* **1992**, *25*, 3838−3842.

(8) Nishide, H.; Kaneko, T.; Nii, T.; Katoh, K.; Tsuchida, E.; Yamaguchi, K. Through-bond and long-range ferromagnetic spin alignment in a π-conjugated polyradical with a poly (phenylenevinylene) skeleton. *J. Am. Chem. Soc.* **1995**, *117*, 548−549.

(9) Nishide, H.; Kaneko, T.; Nii, T.; Katoh, K.; Tsuchida, E.; Lahti, P. M. Poly (phenylenevinylene)-attached phenoxyl radicals: ferromagnetic interaction through planarized and π-conjugated skeletons. *J. Am. Chem. Soc.* **1996**, *118*, 9695−9704.

(10) Takahashi, M.; Nakazawa, T.; Tsuchida, E.; Nishide, H. Poly(4-diphenylaminium-1, 2-phenylenevinylene): a high-spin and durable polyradical. *Macromolecules* **1999**, *32*, 6383−6385.

(11) Nishide, H. High-spin alignment in π-conjugated Polyradicals: A Magnetic polymer. *Adv. Mater.* **1995**, *7*, 937−941.

(12) Miyasaka, M.; Yamazaki, T.; Tsuchida, E.; Nishide, H. Regioregular polythiophene with pendant phenoxyl radicals: a new high-spin organic polymer. *Macromolecules* **2000**, *33*, 8211−8217.

(13) Miyasaka, M.; Yamazaki, T.; Nishide, H. Poly(3-phenylgalvinoxylthiophene). A new conjugated polyradical with high spin concentration. *Polym. J.* **2001**, *33*, 849.

(14) Wang, P.; Lin, S.; Lin, Z.; Peeks, M. D.; Van Voorhis, T.; Swager, T. M. A Semiconducting Conjugated Radical Polymer: Ambipolar Redox Activity and Faraday Effect. *J. Am. Chem. Soc.* **2018**, *140*, 10881−10889.

(15) Eimura, H.; Umeta, Y.; Tokoro, H.; Yoshio, M.; Ohkoshi, S. I.; Kato, T. Self-assembled fibers containing stable organic radical moieties: alignment and magnetic properties in liquid crystals. *Chem. - Eur. J* **2016**, *22*, 8872−8878.

(16) Goto, H. Doping-dedoping-driven optic effect of π-conjugated polymers prepared in cholesteric-liquid-crystal electrolytes. *Phys. Rev. Lett.* **2007**, *98*, No. 253901.

(17) Yoneyama, H.; Kawabata, K.; Tsujimoto, A.; Goto, H. Preparation of iridescent-reflective poly (furan-co-phenylene) s by

electrochemical polymerization in a cholesteric liquid crystal medium. *Electrochem. Commun.* **2008**, *10*, 965−969.

(18) Kawabata, K.; Takeguchi, M.; Goto, H. Optical activity of heteroaromatic conjugated polymer films prepared by asymmetric electrochemical polymerization in cholesteric liquid crystals: structural function for chiral induction. *Macromolecules* **2013**, *46*, 2078−2091.

(19) Goto, H. Vortex fibril structure and chiroptical electrochromic effect of optically active poly (3, 4-ethylenedioxythiophene)-(PEDOT*) prepared by chiral transcription electrochemical polymerisation in cholesteric liquid crystal. *J. Mater. Chem.* **2009**, *19*, 4914−4921.

(20) Kawashima, H.; Kawabata, K.; Goto, H. Intramolecular charge transfer (ICT) of a chiroptically active conjugated polymer showing green colour. *J. Mater. Chem. C* **2015**, *3*, 1126−1133.

(21) Bidan, G.; Guillerez, S.; Sorokin, V. Chirality in regioregular and soluble polythiophene: an internal probe of conformational changes induced by minute solvation variation. *Adv. Mater.* **1996**, *8*, 157−160.

(22) Hattori, S.; Vandendriessche, S.; Koeckelberghs, G.; Verbiest, T.; Ishii, K. Evaporation rate-based selection of supramolecular chirality. *Chem. Commun.* **2017**, *53*, 3066−3069.

(23) Wang, P.; Jeon, I.; Lin, Z.; Peeks, M. D.; Savagatrup, S.; Kooi, S. E.; Voorhis, V. T.; Swager, T. M. Insights into magneto-optics of helical conjugated polymers. *J. Am. Chem. Soc.* **2018**, *140*, 6501−6508.

(24) Goto, H. Magneto-optically active polythiophene derivatives bearing a stable radical group from achiral monomers by polycondensation in cholesteric liquid crystal. *Polymer* **2008**, *49*, 3619−3624.

(25) Innami, Y.; Kiebooms, R. H.; Koyano, T.; Ichinohe, M.; Ohkawa, S.; Kawabata, K.; Kawamatsu, M.; Matsuishi, K.; Goto, H. Synthesis of a low-bandgap polymer bearing side groups containing phenoxy radicals. *J. Mater. Sci.* **2011**, *46*, 6556.

(26) Gierke, W.; Harrer, W.; Kibste, B.; Kurreck, H.; Reusch, J. Übergalvinole und galvinoxyle, ii epr-hfs-undelektronen-spektroskopischeuntersuchungvon galvinoxyl-mehrspinsystemen. *Z. Naturforsch., B: J. Chem. Sci.* **1976**, *31*, 965−973.

(27) Yamamoto, T.; Hayashi, H. π-Conjugated soluble and fluorescent poly (thiophene-2,5-diyl)s with phenolic, hindered phenolic and p-$C_6H_4OCH_3$ substituents. Preparation, optical properties, and redox reaction. *J. Polym. Sci., Part A: Polym. Chem.* **1997**, *35*, 463−474.

(28) Hayashi, H.; Yamamoto, T. Synthesis of regioregular π-conjugated poly (thienyleneethynylene) with a hindered phenolic substituent. *Macromolecules* **1997**, *30*, 330−332.

(29) Li, J. Y.; Chen, C. Y.; Lee, C. P.; Chen, S. C.; Lin, T. H.; Tsai, H. H.; Ho, K. C.; Wu, C. G. Unsymmetrical squaraines incorporating the thiophene unit for panchromatic dye-sensitized solar cells. *Org. Lett.* **2010**, *12*, 5454−5457.

(30) Berova, N.; Nakanishi, K. In *Circular Dichroism: Principles and Applications*, 2nd ed.; Berova, N., Nakanishi, K., Woody, R. E., Eds.; Wiley-VCH: NY, 2000; p 338.

(31) Johnston, D. C. Magnetic structure and magnetization of helical antiferromagnets in high magnetic fields perpendicular to the helix axis at zero temperature. *Phys. Rev. B* **2017**, *96*, No. 104405.

(32) Fang, S.; Lee, M.-S.; Hrovat, D. A.; Borden, W. T. Ab Initio calculations show why m-phenylene is not always a ferromagnetic coupler. *J. Am. Chem. Soc.* **1995**, *117*, 6727−6731.

(33) Kato, S.; Morokuma, K.; Feller, D.; Davidson, E. R.; Borden, W. T. Ab initio study of *m*-benzoquinodimethane. *J. Am. Chem. Soc.* **1983**, *105*, 1791.

(34) Demus, D.; Richter, L. *Texture of Liquid Crystals*; Verlag Chemie: Weinheim, NY, 1978; p 49.

(35) Uchida, M.; Onose, Y.; Matsui, Y.; Tokura, Y. Real-space observation of helical spin order. *Science* **2006**, *311*, 359.